Wind and Structures, *Vol. 21, No. 1 (2015) 85-103*
DOI: http://dx.doi.org/10.12989/was.2015.21.1.085

An empirical model for amplitude prediction on VIV-galloping instability of rectangular cylinders

Huawei Niu[*1], Shuai Zhou[1,2a], Zhengqing Chen[1] and Xugang Hua[1]

[1]*Wind Engineering Research Center of Hunan University, Changsha, Hunan, China*
[2]*China Railway Eryuan Engineering Group Co.Ltd, Chengdu, Sichuan, China*

(Received October 28, 2014, Revised May 4, 2015, Accepted May 8, 2015)

Abstract. Aerodynamic forces of vortex-induced vibration and galloping are going to be coupled when their onset velocities are close to each other, which will induce the cross-wind amplitudes of the structures increased continuously with ever-increasing wind velocities. The main purpose of the present work is going to propose an empirical formula to predict the response amplitude of VIV-galloping interaction. Firstly, two typical mathematical models for the coupled oscillations, i.e., Tamura & Shimada model and Parkinson & Corless model are comparatively summarized. Then, the key parameter affecting response amplitude is determined through comparative numerical simulations with Tamura & Shimada model. For rectangular cylinders with the side ratio from 0.5 to 2.5, which are actually prone to develop the VIV and galloping induced interaction responses, an empirical amplitude prediction formula is proposed after regression analysis on comprehensively collected experimental data with the predetermined key parameter.

Keywords: rectangular cylinders; VIV-Galloping interaction; amplitude prediction; empirical model

1. Introduction

Rectangular cylinders are typical bluff bodies, which are prone to different types of aerodynamic instabilities, depending on the side ratio, such as vortex-induced vibration (VIV) and transverse galloping. VIV is caused by the resonance of the transverse force due to alternative vortex shedding, which is characteristic by amplitude limitation to the order of one cylinder diameter, and occur only in a restricted range of oncoming velocities. The onset velocity of the typical lock-in can be effectively determined by Strouhal law, and the amplitude of vibration depends on the mass ratio and structural damping. VIV is a heat point in the research fields of wind induced vibrations, large efforts on this topic had been done, which are comprehensively reviewed by Bearman (1984), Sarpkaya (1979, 2004), Matsumoto (1999), Williamson and Govardhan (2008). The researches on amplitude estimation are also widely expanded for decades, see e.g., Skop and Griffin (1973), Tamura (1983), Hemon (1999), Govardhan and Williamson (2006) and Marra *et al.* (2011).

By contrast, transverse galloping is caused by a self-excitation due to wind action. Den Hartog

*Corresponding author, Ph.D., E-mail: niuhw@hnu.edu.cn
[a] Ph.D. Student, E-mail: 344953076@qq.com

http://www.techno-press.org/?journal=was&subpage=8 ISSN: 1226-6116 (Print), 1598-6225 (Online)

(Den Hartog 1932) provided an effective way to determine the onset velocity of the galloping instability. The quasi-steady galloping theory is reasonably established on the basis of neglecting unsteady effects, which means the different vibration periods of different amplitudes are taken as only the matters of the varying of relative wind attack angles between structures and approaching flow. Parkinson and Brooks (1961) used polynomials to fit the drag and lift force coefficients curves before expressing the galloping aerodynamic force with limited terms of Taylor series, and the experimental results were reported to be in good agreements with theoretical predictions. In the last five decades, galloping instability of rectangular cylinders were studied by Parkinson and Smith (1964), Parkinson (1965), Bearman *et al.* (1987), Hortmanns and Ruscheweyh (1997), Luo *et al.* (2003), Macdonald and Larose (2006), Gjelstrup and Georgakis (2011), Joly *et al.* (2012), Names *et al.* (2012), etc.

To rectangular cylinders, both VIV and galloping are possible, and there are two major differences between them. Firstly, the response amplitude of galloping would never limited only to be one diameter of cylinder as VIV, which is actually observed to be even 100 times more, for example the transmission lines covered with ice of certain shape. Secondly, the occurring wind velocity ranges of galloping are typically for all speeds above the critical velocity, whereas the VIV is well known to be limited in the lock-in. According to Eurocode 1 (EN 1991-1-4,2010), if the ratio of the galloping to the VIV onset wind speed is either larger than 1.5 or lower than 0.7, the two phenomena can be considered separately. Nevertheless, some experimental data challenged this statement (see e.g., Hansen 2013, Mannini *et al*. 2014). To the slender structural elements with rectangular cross sections, however, when the onset velocities of VIV and galloping are very close, the aerodynamic forces of VIV and galloping are prone to be coupled, therefore interaction between the two phenomena can be expected. Then structural response appears to be a novel form which is beyond the single VIV or galloping style. As reported by many investigations (Parkinson 1965, Borri *et al*. 2012, Mannini *et al*. 2013, Mannini *et al*. 2014, etc.), the oscillations will start at the onset velocities which are always decided by Strouhal law or quasi-steady galloping theory, the response amplitude increase almost linearly with wind velocity, no signs of setback.

In fact, the interaction cases of VIV and galloping are very common in the slender rectangular cylinders because of their bluff aerodynamic shapes. For the practical engineering applications, it will be very convenient if there is an empirical formula to predict the amplitude of the VIV-galloping instability, just like Griffin Plot for VIV (Skop and Griffin 1973). While many investigations have been carried out for studying the response amplitude due to combined VIV and galloping, a simple model is still absent for practical applications purpose even under a certain pre-determined conditions. So the main purpose of the present work is trying to build an empirical model, based on a lot of collected experimental data and wind tunnel tested data performed by present work, by curve fitting.

2. Materials and methods

2.1 Characteristics of the interaction effects

Fig. 1 is showing a group of experimental curves of rectangular cylinders in different aspect ratios, which performed by Parkinson and Brooks (1961). In this figure, the x-axis is the dimensionless wind velocity, while the ordinate is the dimensionless amplitude response. It is

worth noting the response curves of rectangular cylinders whose aspect ratios *d/h* are above 0.75, the amplitudes are observed to be generally increased as linear fashion with wind velocities. It is also reported that cylinders are dominantly vibrating at the natural frequencies and the time history of each case are keeping steady in this whole experimental group.

Fig. 2 is showing another typical group of results on VIV and galloping interaction induced oscillations, which are presented by Corless and Parkinson (1988). Vibration curves of the same square cylinder at different damping levels are presented, and the experimental results coincide with numerical results relatively well. While the onset velocities are different for the three cases, the rate of change of response amplitude with respect to the wind velocity for each case are observed to be almost the same.

Many more results can be found that VIV and galloping interaction induced vibration curves of rectangular cylinders like Figs. 1 and 2 in the foregoing researches. The main characteristics of the oscillation curves maybe concluded as following two points, firstly, the onset velocities are always determined by Strouhal law or quasi-steady galloping theory; secondly, the shape of the curves are showing linearly increased behaviors, which means the rate of change of the amplitude with respect to wind velocity is constant after the starting point, although the values are varying with aspect ratios. That's to say, if we can appropriately the slope of the response curve, the amplitude prediction may be straightforwardly made. Therefore, we define a new parameter S_L as Eq. (1) to present this parameter.

$$S_L = \frac{\Delta Y}{\Delta U_r} \tag{1}$$

where, ΔY is the increment of amplitude; $Y=A/D$ is the dimensionless amplitude response; ΔU_r is the increment of wind velocity associate with increased amplitude; $U_r=V/(f_vD)$ is the normalized wind velocity; V is oncoming wind velocity; f_v is the dominant oscillating frequency.

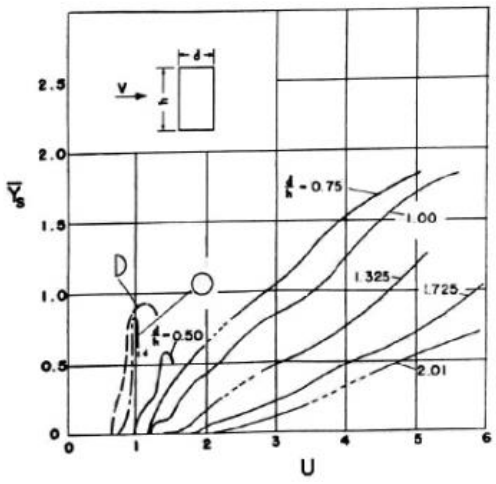

Fig. 1 Experimental curves of amplitude versus dimensionless wind velocity for different aspect ratio rectangular cylinders (Parkinson and Brooks 1961)

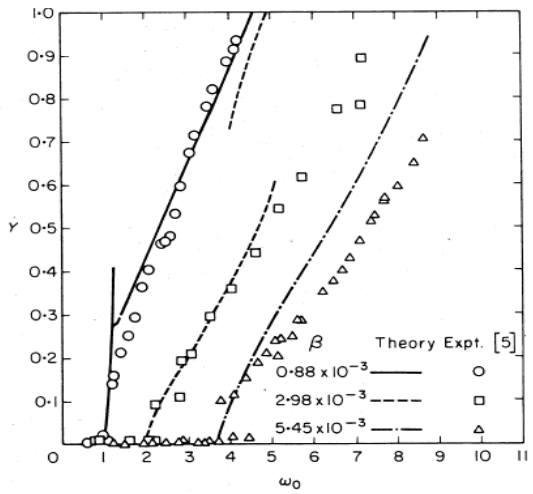

Fig. 2 Comparision on amplitude responses of three levels of system damping between simulation and experimental results (Corless and Parkinson, 1988, Bearman *et al*. 1987)

2.2 Mathematical models

The mathematical modeling on interaction effects between VIV and galloping could be classified into two main branches, one is proposed by Corless and Parkinson (1988), which is characterized by parametrical mathematical fitting on measured vibration results; the other one is Tamura and Matsui model (Tamura and Matsui 1979), which pay more attention on the physical meanings of parameters. And the common point of these two models is that both they are based on the quasi-steady galloping theory with one kind of VIV model to form the coupled VIV and galloping model.

2.2.1 Parkinson and Corless model

In order to take into account the effects of vortex shedding force and quasi-steady galloping force, Parkinson and Bouclin (1977) describe the integrated unsteady aerodynamic force acting on a square cylinder by adding the quasi-steady perturbation to the Hartlen-Currie fluid oscillator, then Eq. (2) is obtained.

$$\ddot{Y}+Y=nU^2(C_{FY}+C_L)$$
$$\ddot{C}_L-G\left\{C_{L0}^2-(4/3)\left(\dot{C}_L/k\right)^2\right\}\dot{C}_L+k^2C_L=H\dot{Y}$$
$$C_{FY}=A_1\cdot\left(\frac{\dot{Y}}{V}\right)^1+A_2\cdot\left(\frac{\dot{Y}}{V}\right)^2+A_3\cdot\left(\frac{\dot{Y}}{V}\right)^3+A_4\cdot\left(\frac{\dot{Y}}{V}\right)^4+A_5\cdot\left(\frac{\dot{Y}}{V}\right)^5+A_6\cdot\left(\frac{\dot{Y}}{V}\right)^6+A_7\cdot\left(\frac{\dot{Y}}{V}\right)^7 \quad (2)$$

where, G, k, H are the constants which are determined by mathematical fitting on the response curves; C_L is the lift coefficient; $\dot{Y}$ is the structural velocity response; n is the mass ratio, defined as the ratio of fluid mass over structural mass of the same unit; C_{FY} represents the quasi-steady galloping aerodynamic force, it is obtained by expanding Taylor series of drag and lift coefficient according to quasi-steady galloping theory, and up to 7^{th} term is proved to be sufficient by many

investigations. The good coincidences between experimental and simulation results demonstrate that this mathematical model can successfully consider the interaction effects of VIV and galloping.

Corless and Parkinson (1988) improved it by adding a new coupling term of $B\ddot{Y}$ into the differential equation in the expectation of considering some effects of cylinder acceleration on the wake vortices. And Facchinettia *et al*. (2004) proved that using acceleration as coupling term is indeed more effective than using displacement or velocity by comparative wind tunnel tests studies. According to Corless and Parkinson (1998), Eq. (2) is modified as

$$\begin{gathered}\ddot{Y}+Y=nU^2(C_{FY}+C_L)\\ \ddot{C}_L-G\left\{C_{L0}^2-(4/3)\left(\dot{C}_L/k\right)^2\right\}\dot{C}_L+k^2C_L=H\dot{Y}+B\ddot{Y}\end{gathered} \tag{3}$$

The differential equations Eq. (1) can be solved by the method of multiple scales. The simulation obtained curves have a good agreement with the experimental results, which show that the effects of VIV could be simply added to the time-averaged position of shear layer to predict the aerodynamic force.

2.2.2 Tamura and Shimada model

There is a main branch in VIV mathematical models research field, they considered the alternatively shedding vortices as an independent oscillator, this oscillator could be interacted with structural vibration to form a combined motion equation, e.g., Birkhoff type VIV model. And the modified Birkhoff type VIV mathematical model on circular cylinders is proposed by Tamura and Matsui (1979), which is characteristically for has taken into account the effects of verified length of the wake-oscillator on aerodynamic forces. The coupled dynamic equation between wake oscillator and circular cylinder motion is expressed as Eq. (4)

$$\begin{gathered}\ddot{\alpha}-2\zeta v\left\{1-\left(4f^2/C_{L0}^2\right)\alpha^2\right\}\dot{\alpha}+v\alpha=-m^*\ddot{Y}-vS^*\dot{Y}\\ \ddot{Y}+\left\{2\eta+n(f+C_D)v/S^*\right\}\dot{Y}+Y=-fmv^2\alpha/S^{*2}\\ C_L=-f\left(\alpha+S^*\dot{Y}/v\right)\end{gathered} \tag{4}$$

where, α is the angular displacement of wake oscillator; Y is the dimensionless transverse displacement of circular cylinder; V is oncoming wind velocity; ζ is wake oscillator damping ratio, $\zeta=1/(2\sqrt{2}*\pi^2)*f/Hr$; $v=U_r/U_s$ is the non-dimensional flow velocity; $U_s=f_vD/St$ is the Strouhal number determined from the critical wind velocity; η is the mechanical damping ratio of structure; f is the parameter which determined by the Magnus effect; Hr is the dimensionless width of the wake oscillator; C_{L0} is the static lift coefficient amplitude for circular cylinders; C_D is the drag coefficient for circular cylinders; m^* is the equivalent mass ratio, $m^*=1/(0.5+Hr)$; S^* is the equivalent Strouhal number. For circular cylinders, the aerodynamic parameters are determined by the previous experiments as following: $m^*=0.625$, $S^*=1.26$, $f=1.16$, $C_D=1.2$. The differential equation Eq. (4) can be solved by Runge-Kutta method, and the numerical results are reported to agree with the experimental results qualitatively and quantitatively (Tamura and Matsui 1979).

For square cylinders, when the onset velocities of VIV and galloping are very close, the oscillation curves are observed to be coupled, Tamura and Shimada (1987) proposed a coupling

mathematical model to consider this interaction effects. Using previously proposed modified Birkhoff type wake oscillator model to consider the vortex shedding force, and quasi-steady perturbation model (Parkinson and Brooks 1961) for galloping aerodynamic force, the coupled mathematical model is established by the superimposing of these two discrete aerodynamic force parts. The detailed processes of constructing the coupled model is as following: expanding the quasi-steady galloping force C_{FY} by Taylor series and taking the first 7 orders as galloping force, combining the equivalent galloping force into the modified Birkhoff type VIV model, then the coupled mathematical is finally established as Eq. (5)

$$\begin{gathered}\ddot{\alpha}-2\zeta v\left\{1-\left(4f^2/C_{L0}^2\right)\alpha^2\right\}\dot{\alpha}+v\alpha=-m^*\ddot{Y}-vS^*\dot{Y} \\ \ddot{Y}+\left\{2\eta+n(f-A_1)v/S^*-nA_3S^*/v\dot{Y}^2-nA_5\left(S^*/v\right)^3\dot{Y}^4-nA_7\left(S^*/v\right)^5\dot{Y}^6\ldots\right\}\dot{Y}+Y=-fnv^2\alpha/S^{*2} \\ C_L=-\left\{(f-A_1)S^*\dot{Y}/v-A_3\left(S^*\dot{Y}/v\right)^3-A_5\left(S^*\dot{Y}/v\right)^5-\ldots+f\alpha\right\}\end{gathered} \tag{5}$$

where, A_1, A_3, A_5, A_7 are the coefficients of the Taylor series expansions, the meanings of other symbols are the same as mentioned above. The effectiveness of the Tamura-Shimada mathematical model on interaction effects between VIV and galloping is verified by good consistency between theoretical prediction and experimental results, and most importantly, all the parameters in this model have definite physical interpretations.

Since the parameters in the Hartlen-Currie model are mainly a kind of mathematical curves-fitting on experimental results; while all the parameters in the Tamura-Shimada mathematical model have their physical meanings, therefore the later will shed insight into the vibration mechanism. Allison and Corless (1995) also indicate that the mathematical model of the Tamura-Shimada model is more rationally derived than their Hartlen-Currie model.

2.3 The determination of key parameter

As defined before, S_L is the key parameter for predicting amplitude response of coupled VIV and galloping vibrations, here, in this part, we are going to further investigate by numerical simulations on which is the main influence factor of this key parameter.

Regarding which are the potential influencing factors on S_L, the steady vibration history of each wind velocity point should be carefully analyzed, the limit-cycle vibration status of each case means that the total energy absorbing from the oncoming flow are going to balance the energy dissipated by the system damping and maintain the kinetic energy of structure (Vio *et al.* 2007). Therefore, it is reasonable to assume that S_L should be associated with the aspect ratio of the cross section, because it is directly affecting the efficiency of structure on absorbing energy from the approaching flow. On the contrary, structural physical mass, system damping and vibration frequency are the main factor who are affecting the efficiency of energy dissipating, they are deserved to be regarded as potential factors on S_L. Moreover, the Reynolds number is also an important parameter that can't be neglected.

Consequently, the S_L may be assumed as the function of several factors which is shown in Eq. (6)

$$S_L=F\left(n,\eta,f_v,A_F,R,Re\right) \tag{6}$$

where, n is mass ratio; η is mechanical damping ratio of structure; f_v is dominant vibrating frequency, which is basically equaling to the structural natural frequency in VIV and galloping coupled vibrations, so it will be excluded in the dimensionless expressions; A_F is representing the influences of all the fluid parameters, such as f, C_{L0}, H_r .etc; $R=B/D$ is the aspect ratio of rectangular cylinders, the ratio of along wind dimension over cross wind dimension; Re, is Reynolds number, its effect may be combined into the aerodynamic coefficients, i.e., aspect ratio of rectangular cylinders. Therefore, S_L could be further simplified as Eq. (7)

$$S_L=F(n,\eta,A_F,R) \tag{7}$$

2.3.1 The effect of structural parameters

The Tamura-Shimada mathematical model (Eq. (5)) is selected to perform the comparative simulations in this part, because the physical interpretations of each variables could be checked and the whole equation group is more rational derived which is concluded in section 2.2.

First of all, a set of classical data on VIV and galloping interaction is taken here to verify the efficiency of Tamura-Shimada mathematical model. As shown in Fig. 2, the experimental data of square cylinder is provided by Bearman *et al.* (1987), Corless and Parkinson (1988) verified it by their mathematical model. The parametrical details of mass ratio, damping ratio and galloping coefficients are shown in Tables1 and 2. Some other parameters are needed before calculating with the Tamura-Shimada model, where St=0.12 is used for Strouhal number; the fluid parameters i.e. Hr and f are respectively assumed to 1.8 and 1.16, which are the same value as circular cylinder, and their effects will be separately investigated later; amplitude of lift coefficient on a stationary square cylinder C_{L0} is reported by many researchers, C_{L0}=0.7 is basically adopted for calculation. Eq. (5) is solved by Runge-Kutta method, time step is scaled to as small as 0.05, and the longest calculation time is up to 20000 to ensure all the obtained results are steady and reasonable.

Fig. 3 shows the comparison between calculation results and experimental measured data of Bearman .etc, at the low wind velocity range, there is a small range of VIV lock-in appearing in calculation processes but not provided in experimental curves. The differences might be attributed to the error of values of fluid parameters because of lacking the precise experimental results. However, the good agreements of calculation and experiments can be observed after the VIV and galloping interaction starting point. Once again, the Tamura-Shimada model is proved to be efficient on predicting such kind of interaction effects.

Table 1 is a list of parameters, from which we can see the only varying parameter is damping ratio, three different levels separately according to experimental data of Fig. 2. Similarly, we input these parameters into Tamura-Shimada model and solve it by Runge-Kutta method, the results are shown in Fig. 4. Different damping ratios give rise to different oscillation curves, more specifically, higher damping ratios postpone the oscillation starting point; and the same wind velocity point, the higher of damping ratios, the lower of amplitudes will be. However, the most concerned amplitude slope S_L of present work are observed to be basically the same even the significantly changed damping ratios, which means that S_L may not be sensitive with damping.

And in the comparative investigation of mass on amplitude slope S_L, as shown in Fig. 5, the only varying parameter mass ratio are adjusted by double, and S_L are basically the same. Therefore, the similar conclusion as damping ratio can be drawn: S_L is also not sensitive with mass.

Table 1 Investigation on damping ratio

Structural parameters		Fluid parameters			Aerodynamic parameters			
Mass ratio (n)	Damping ratio (η)	Wake oscillator parameter (Hr)	Magnus effect (f)	Lift coefficient (C_{L0})	A_1	A_3	A_5	A_7
4.7e-4	0.88e-3 2.98e-3 5.45e-3	1.8	1.16	0.70	4.87	421	1.70e4	1.94e5

Table 2 Investigation on mass ratio

Structural parameters		Fluid parameters			Aerodynamic parameters			
Mass ratio (n)	Damping ratio (η)	Wake oscillator parameter (Hr)	Magnus effect (f)	Lift coefficient (C_{L0})	A_1	A_3	A_5	A_7
0.5*4.7e-4 4.7e-4 2*4.7e-4	2.98e-3	1.8	1.16	0.70	4.87	421	1.70e4	1.94e5

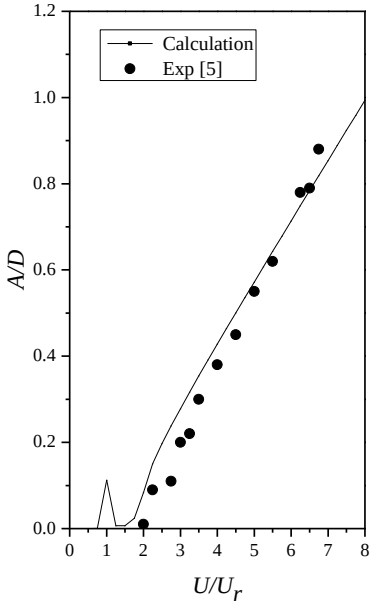

Fig. 3 Comparison between Bearman's experimental data and calculation results

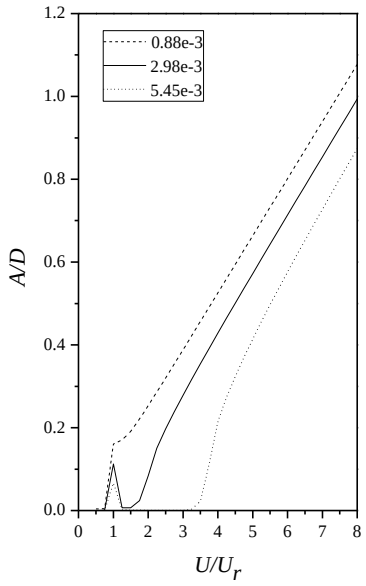

Fig. 4 The effects of damping on amplitude response

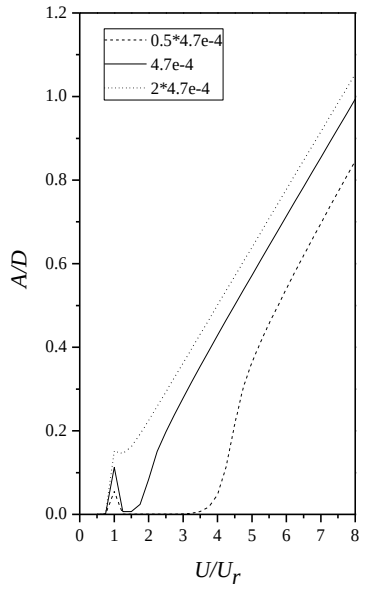

Fig. 5 The effects of mass on amplitude response

2.3.2 The effect of fluid parameters

Here, in this part, we are going to check the effects of fluid parameters (i.e., f, C_{L0}, H_r) on amplitude response parameter S_L by the Tamura-Shimada model. Three cases are formed due to the

main principle of changing only one parameter in each case. The calculating parameters of each case are separately listed from Table 3 to Table 5. The way to vary parameter values in each case is unified as scaling 2 times and 0.5 times on the basis of a standard value, then three different values are obtained in each case.

Similarly, the Tamura-Shimada models are solved by Runge-Kutta method, simulation curves are obtained as shown in Fig. 6 to Fig. 8. It can be observed from Fig. 6 that the large extent of changing fluid parameter *Hr* did not bring any obvious changes on simulation results, simulation curves are almost coincided both in low wind range VIV and high wind interaction responses. The effects of fluid parameters *f* and C_{L0} on response amplitude are shown in Figs. 7 and 8 respectively. While different values of each parameter causes significant response variation in VIV response amplitude, the coupled VIV and galloping response are basically the same. Therefore it is concluded that w the fluid parameters *f*, C_{L0}, H_r are not the main affecting factors on response slope S_L.

Table 3 Investigation on *Hr*

Structural parameters		Fluid parameters			Aerodynamic parameters			
Mass ratio (n)	Damping ratio (η)	Wake oscillator parameter (Hr)	Magnus effect (f)	Lift coefficient (C_{L0})	A_1	A_3	A_5	A_7
4.7e-4	2.98e-3	0.5*1.8 1.8 2*1.8	1.16	0.70	4.87	421	1.70e4	1.94e5

Table 4 Investigation on *f*

Structural parameters		Fluid parameters			Aerodynamic parameters			
Mass ratio (n)	Damping ratio (η)	Wake oscillator parameter (Hr)	Magnus effect (f)	Lift coefficient (C_{L0})	A_1	A_3	A_5	A_7
4.7e-4	2.98e-3	1.8	0.5*1.16 1.16 2*1.16	0.70	4.87	421	1.70e4	1.94e5

Table 5 Investigation on C_{L0}

Structural parameters		Fluid parameters			Aerodynamic parameters			
Mass ratio (n)	Damping ratio (η)	Wake oscillator parameter (Hr)	Magnus effect (f)	Lift coefficient (C_{L0})	A_1	A_3	A_5	A_7
4.7e-4	2.98e-3	1.8	1.16	0.5*0.70 0.70 2*0.70	4.87	421	1.70e4	1.94e5

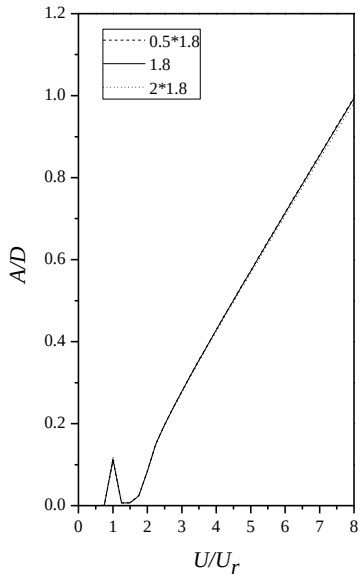

Fig. 6 The effects of wake oscillator parameter *Hr* on amplitude response

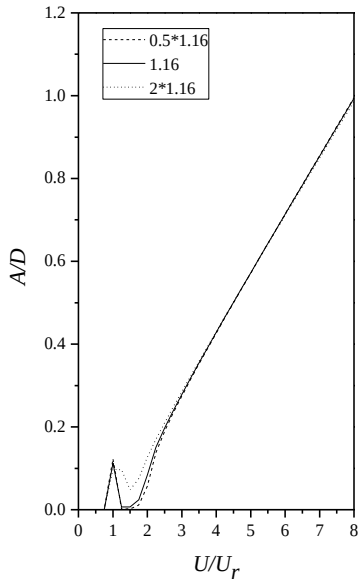

Fig. 7 The effects of Magnus parameter *f* on amplitude response

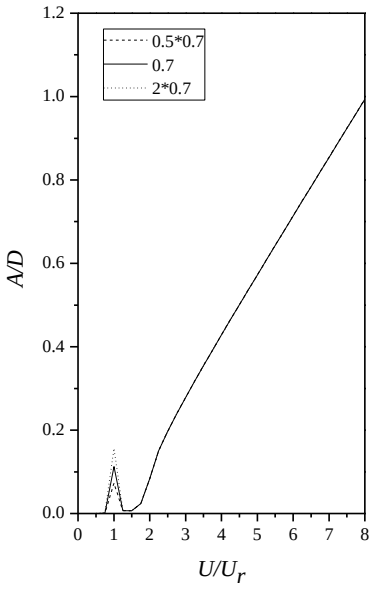

Fig. 8 The effects of lift coefficient C_{L0} on amplitude response

Table 6 Investigation on quasi-steady galloping coefficients

Structural parameters		Fluid parameters			Aerodynamic parameters			
Mass ratio (n)	Damping ratio (η)	Wake oscillator parameter (Hr)	Magnus effect (f)	Lift coefficient (C_{L0})	A_1	A_3	A_5	A_7
4.7e-4	2.98e-3	1.8	1.16	0.70	4.87 1.30	421 315	1.70e4 5.70e4	1.94e5 1.72e5

2.3.3 The effect of aerodynamic parameters

The effect of aerodynamic parameters A_1, A_3, A_5… A_N on amplitude response parameter S_L is numerically studied in this part. Two cases are selected, one is square cylinder, the aspect ratio of cross section is definitely to be 1.0, and the aerodynamic parameters A_1, A_3, A_5, A_7 are 4.87, 421, 1.70e4, 1.94e5 respectively according to the former researchers' report (Corless and Parkinson, 1988); the other one is a rectangular cylinder whose aspect ratio is 1.4, the aerodynamic parameters are correspondingly determined to be as 1.30, 315, 5.70e4, 1.72e5 by static force coefficients wind tunnel tests in present work.

Numerical simulations are performed under Tamura-Shimada model with the same processes as before, comparative results curves are plotted in Fig. 9. As we can see, two curves exhibit the obvious differences on interaction responses stages not only at starting point but for amplitude increasing slope S_L. The value of S_L of square cylinder is calculated to be 0.1385, while the result of the other rectangular cylinder is 0.0935, the deviation between them is over 40%. Therefore, we may conclude that aerodynamic parameters are the main affecting factors on amplitude slope S_L. It is worth noting that for rectangular cylinders, aerodynamic parameters are only determined by

aspect ratio, so we can further conclude that the aspect ratio of rectangular cylinder is actually the key factor for S_L.

3. Results and discussions

The key parameter S_L is found to be only associated with aspect ratio ($R=B/D$) of rectangular cylinders through comparative numerical simulations in last part. For rectangular cylinders who are suffered from VIV and galloping coupled oscillations, S_L is going to be uniformly determined in this part by regression analysis on $R=B/D$ with comprehensively collected experimental data.

3.1 The collected data

Table 7 is the list of collected experimental data of rectangular cylinders on interaction effects between VIV and galloping, 26 cases in total. The corresponding vibration curves of 26 cases are separately presented in Fig. 10, the high magnitude of mathematical fitting deviation R^2 for all cases are clearly shown, and the obviously linear relationship between normalized wind velocities and dimensionless amplitudes are presented.

For each case, the aspect ratio, mass, damping, predicted onset velocity ratio of galloping over VIV, S_L and dimensionless onset velocity of interaction vibration are presented in Table 7, which shows the good representative for collected data: aspect ratio range is varying from 0.71 to 2.49; the predicted onset velocity ratio of galloping over VIV is distributing from 0.1 to 8.4; and most importantly, S_L , i.e., the slope of increased amplitude over increased wind velocity, obtained by the least square linear fitting on vibration curves of collected data (See Fig. 10), is ranging from 0.011 to 0.104, which is showing the promising signs for the establishment of empirical amplitude prediction formula.

Regarding the onset velocities of interaction effects, on the basis of Table 7, the general conclusion may be drawn as following: the dimensionless onset velocity is controlled by VIV when $0.2 < V_g/V_v < 5$, then U_0 should be floating at 1.0; and the onset velocity will be controlled by galloping when $V_g/V_v > 5$ or $V_g/V_v < 0.2$, U_0 appears to be determined by quasi-steady galloping theory.

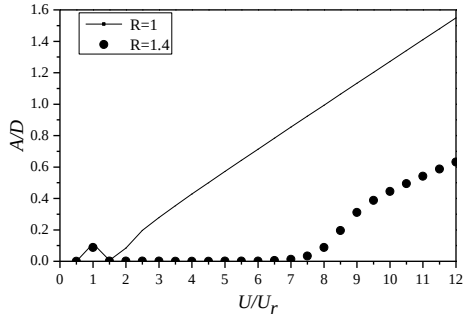

Fig. 9 The effects of aspect ratio on amplitude response

Table 7 Main parameters and fitting data

No.	*R=B/D*	*η/n*	V_g/V_v	S_L	U_0
Case 1	1.40	2.2	2.4	0.037	1.0
Case 2	1.40	2.7	3.0	0.029	1.0
Case 3	1.40	2.7	3.1	0.032	1.0
Case 4	1.40	3.7	4.1	0.030	0.8
Case 5	1.40	4.0	4.5	0.023	0.9
Case 6	1.40	2.0	2.2	0.026	1.1
Case 7	1.40	0.1	0.1	0.104	0.4
Case 8	1.40	1.6	3.0	0.024	0.7
Case 9	1.31	0.7	1.4	0.048	0.7
Case 10	2.00	1.0	3.0	0.017	1.2
Case 11	2.00	1.1	1.6	0.016	0.6
Case 12	2.00	1.7	2.6	0.019	0.6
Case 13	2.00	2.2	3.3	0.021	0.7
Case 14	2.00	2.4	3.6	0.019	0.6
Case 15	1.00	1.3	1.1	0.048	1.1
Case 16	1.00	1.8	1.5	0.045	1.0
Case 17	1.50	7.6	8.4	0.021	2.9
Case 18	1.50	1.3	1.4	0.024	2.0
Case 19	0.76	0.7	1.6	0.068	0.6
Case 20	0.71	1.6	5.1	0.075	4.7
Case 21	0.75	-	< 1	0.064	0.9
Case 22	1.00	-	< 1	0.026	0.9
Case 23	1.33	-	< 1	0.019	0.9
Case 24	1.73	-	< 1	0.015	0.9
Case 25	2.01	-	< 1	0.011	0.9
Case 26	2.49	-	< 1	0.016	0.9

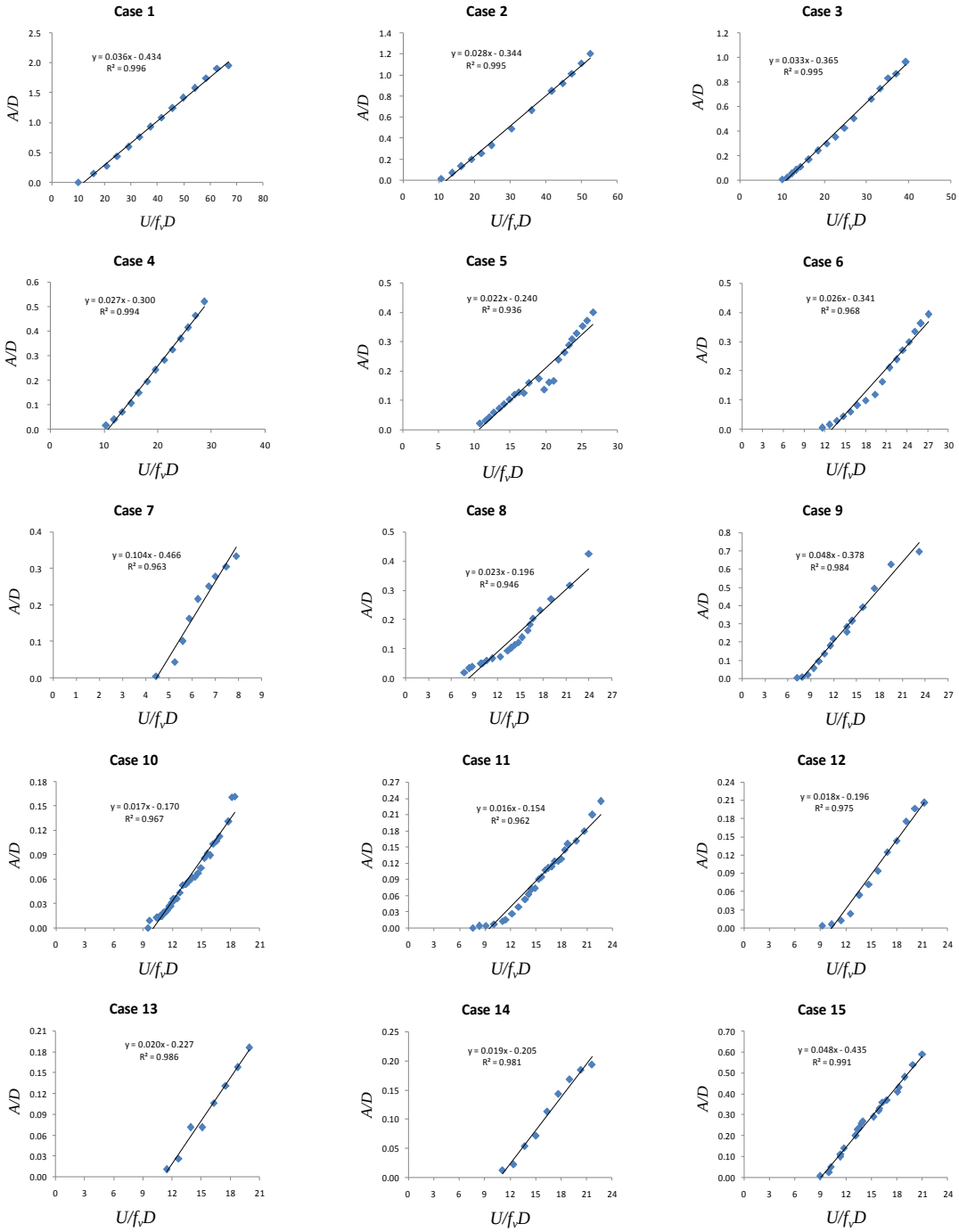
Case 1
y = 0.036x - 0.434
R² = 0.996
Case 2
y = 0.028x - 0.344
R² = 0.995
Case 3
y = 0.033x - 0.365
R² = 0.995
Case 4
y = 0.027x - 0.300
R² = 0.994
Case 5
y = 0.022x - 0.240
R² = 0.936
Case 6
y = 0.026x - 0.341
R² = 0.968
Case 7
y = 0.104x - 0.466
R² = 0.963
Case 8
y = 0.023x - 0.196
R² = 0.946
Case 9
y = 0.048x - 0.378
R² = 0.984
Case 10
y = 0.017x - 0.170
R² = 0.967
Case 11
y = 0.016x - 0.154
R² = 0.962
Case 12
y = 0.018x - 0.196
R² = 0.975
Case 13
y = 0.020x - 0.227
R² = 0.986
Case 14
y = 0.019x - 0.205
R² = 0.981
Case 15
y = 0.048x - 0.435
R² = 0.991
A/D
U/fvD

Continued-

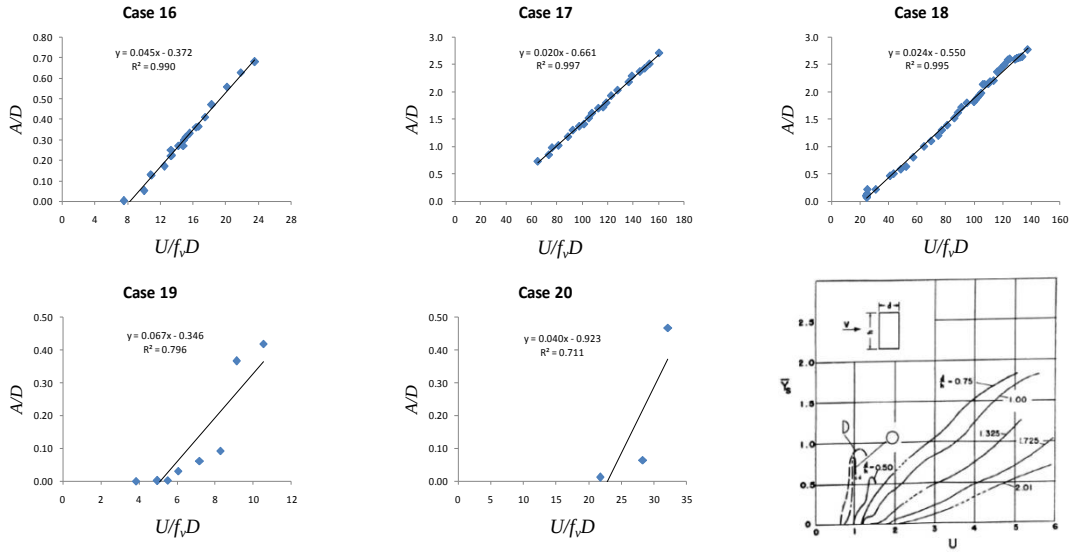

Fig. 10 The plot lists on the normalized wind velocity vs. dimensionless amplitude and the corresponding linear fitting equations

3.2 Empirical formula

The fitting curve between aspect ratio $R=B/D$ of rectangular cylinders and linear slope S_L of amplitude response is obtained by polynomial fitting method as shown in Fig. 11, from which we can get the mathematical expression of S_L on $R=B/D$.

Because of the onset velocity could be reasonably obtained by Strouhal law, then finally, the empirical formula to predict the amplitude of coupled VIV and galloping response can be obtained as Eq. (8)

$$\frac{A}{D}=\left(-0.016\cdot R^3+0.101\cdot R^2-0.222\cdot R+0.182\right)\cdot\left(U_r-U_0\right) \tag{8}$$

Where, A/D is the dimensionless amplitude response; R is the aspect ratio of rectangular cylinders; $U_r=V/(f_vD)$ is the normalized wind velocity where we want predict the amplitude response; $U_0=0.9/St$ is onset velocity according to the generally summarized data.

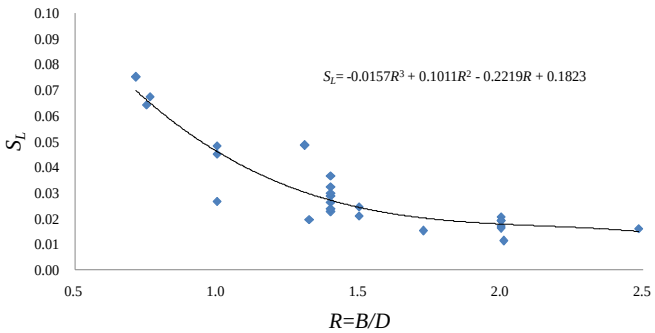

Fig. 11 The mathematical fitting between R and S_L based on the collected data

However, there are still several limitations for the use of this formula on amplitude prediction of rectangular cylinders should be noted:

Firstly, due to the limited collected data during mathematical fitting process, the aspect ratio of rectangular cylinders should be confined to the range of $0.5< R=B/D < 2.5$; secondly, there are few points in Fig. 11 observed to be scattered in the mathematical fitting between S_L and R, more data is required in the future investigations to improve the accuracy of this empirical curve; and more importantly ,this empirical formula is only applicable for the VIV-galloping coupled cases.

4. Conclusions

The coupled oscillations between VIV and galloping of rectangular cylinders are observed by many researchers; mathematical models which have taken into account the combined effects of VIV and galloping are also separately presented, mainly, Tamura & Shimada model and Corless & Parkinson model.

The interaction oscillations are characterized by: firstly, there will be an onset velocity which is decided by Strouhal law or quasi-steady galloping theory; secondly, the amplitude response curves are always observed to be linearly increased accompanied by wind velocities. Therefore, it is reasonable to propose an empirical amplitude estimation formula on the basis of careful research on onset velocity and amplitude increasing slope S_L .

Tamura & Shimada model is taken as the main model to perform comparative numerical simulations in present work, large amount of simulation works indicate that S_L is only associated with aspect ratio of rectangular cylinders. On the basis of comprehensively collected experimental data on interaction oscillations, S_L is determined by regression analysis, an empirical formula to predict the amplitude response of interaction oscillations of rectangular cylinders is finally proposed.

However, more efforts are need to improve the accuracy of this empirical formula, as several points are observed to be scattered during the mathematical fitting processes.

Acknowledgements

The authors are gratefully acknowledging the support of Natural Science Foundation of China under the Grant Nos. 51478181, 50908085 and 91215302. Special thanks to Prof. Tamura of Tokyo Polytechnic University and Prof. Borri of University of Florence for their patient and valuable comments on this paper.

References

Allison E, A.M. and Corless, R.M. (1995), "Prediction of closed-loop hysteresis with a flow-induced vibration model", *Proceedings of the 15th Canadian Congress of Applied Mechanics*, Victoria, Canada, May.

Bearman, P.W. (1984), "Vortex shedding from oscillating bluff bodies", *Annu. Rev. Fluid Mech.*, **16**(1), 195-222.

Bearman, P.W., Gartshore, I.S., Maull, D.J. and Parkinson, G.V. (1987), "Experiments on flow-induced

vibration of a square section cylinder", *J. Fluids Struct.*, **1**(1), 19-34.
Borri, C., Zhou, S. and Chen, Z. (2012), "Coupling investigation on vortex-induced vibration and galloping of rectangular cylinders", *Proceedings of the Seventh International Colloquium on Bluff Body Aerodynamics and Applications*, Shanghai, China, September.
Corless, R.M. and Parkinson, G.V. (1988), "A model of the combined effects of vortex-induced oscillation and galloping", *J. Fluids Struct*., **2**(3), 203-220.
Den Hartog, J.P. (1932), "Transmission-line vibration due to sleet", *AIEE*, **51**, 1074-1086.
EN 1991-1-4 (2010), Eurocode 1-Actions on Structures, Parts 1-4: General Actions-Wind Actions.
Facchinetti, M.L., Langrea, E.de. and Biolley, F. (2004), "Coupling of structure and wake oscillators in vortex-induced vibrations", *J. Fluids Struct*., **19**(2) ,123-140
Garrett, J.L. (2003), *Flow-induced vibration of elastically supported rectangular cylinders*, Ph.D. Dissertation, Iowa State University, Ames.
Govardhan, R.N. and Williamson, C.H.K. (2006), "Defining the 'modified griffin plot' in vortex-induced vibration: revealing the effect of Reynolds number using controlled damping", *J. Fluid Mech*., **561**,147-180.
Gjelstrup, H. and Georgakis, C.T. (2011), "A quasi-steady 3 degree-of-freedom model for the determination of the onset of bluff body galloping instability", *J. Fluids Struct*., **27**(7), 1021-1034
Hansen, S.O. (2013), "Wind loading design codes", Fifty Years of Wind Engineering —Prestige Lectures from the Sixth European and African Conference on Wind Engineering, Cambridge, UK, July.
Hortmanns, M. and Ruscheweyh, H. (1997), "Development of a method for calculating galloping amplitudes considering nonlinear aerodynamic coefficients measured with the forced oscillation method", *J. Wind Eng. Ind. Aerod*., **69-71**, 251-261.
Hemon, P. (1999), "An improvement of time delayed quasi-steady model for the oscillations of circular cylinders in cross-flow", *J. Fluids Struct*., **13**(3), 291-307.
Joly, A., Etienne, S. and Pelletier, D. (2012), "Galloping of square cylinders in cross-flow at low Reynolds numbers", *J. Fluids Struct*., **28**, 232-243.
Luo, S.C., Chew, Y.T. and Ng, Y.T. (2003), "Hysteresis phenomenon in the galloping oscillation of a square cylinder", *J. Fluids Struct*., **18**(1), 103-118.
Macdonald, H.G. and Larose, G.L. (2006), "A unified approach to aerodynamic damping and drag/lift instabilities, and its application to dry inclined cable galloping", *J. Fluids Struct*., **22**(2), 229-252.
Mannini, C., Marra, A.M., Massai, T. and Bartoli, G. (2013), "VIV and galloping interaction for a 3:2 rectangular cylinder", *Proceedings of the 6th European and African Conference on Wind Engineering*, Cambridge, UK, July.
Mannini C., Marra A.M. and Bartoli G. (2014), "VIV–galloping instability of rectangular cylinders: Review and new experiments", *J. Wind Eng. Ind. Aerod*., **132**, 109-124.
Marra, A.M., Mannini, C. and Bartoli, G. (2011), "Van der Pol-type equation for modeling vortex-induced oscillations of bridge decks", *J. Wind Eng. Ind. Aerod*., **99**(6-7), 776-785.
Matsumoto, M. (1999), "Vortex shedding of bluff bodies: a review", *J. Fluids Struct*., **13**(7-8), 791-811.
Names, A., Zhao, J., Lo Jacono, D. and Sheridan, J. (2012), "The interaction between flow-induced vibration mechanisms of a square cylinder with varying angles of attack", *J. Fluid Mech*., **710**, 102-130.
Parkinson, G.V. and Bouclin, D. (1977), "Hydroelastic oscillation of square cylinders", International Research Seminar on Safety of Structures under Dynamic Loading, Trondheim, Norway, June.
Parkinson, G.V. and Brooks, N.P.H. (1961), "On the aeroelastic instability of bluff cylinders", *J. Appl. Mech. - T ASME*, **28**(2), 252-258.
Parkinson, G.V. and Smith, J.D. (1964), "The square cylinder as an aeroelastic non-linear oscillator", *Quart. J. Mech. Appl. Math*., **17**(2), 225-239.
Parkinson, G.V. (1965), "Aeroelastic galloping in one degree of freem", Wind Effects on Buildings and Structures: Proceedings of the Conference Held at the National Physical Laboratory, Teddington, UK, June.
Parkinson, G.V. and Wawzonak, M.A. (1981), "Some consideration of combined effects of galloping and vortex resonance", *J. Wind Eng. Ind. Aerod*., **8**(1-2), 135-143.

Skop, R.A. and Griffin, O.M. (1973), "A model for the vortex-excited resonant response of bluff cylinders", *J. Sound Vib*., **27**(2), 225-233.
Sarpkaya, T. (1979), "Vortex-induced oscillations: a selective review", *J. Appl. Mech*. - *T ASME*, **46**(2), 241-258.
Sarpkaya, T. (2004), "A critical review of the intrinsic nature of vortex-induced vibrations", *J. Fluids Struct*., **19**(4), 389-447.
Tamura, Y. and Matsui, G. (1979), "Wake-oscillator model of vortex-induced oscillation of circular cylinder", *Proceedings of the 5th international conference on wind engineering*, Fort Collins, USA, July.
Tamura, Y. (1983), "Mathematical model for vortex-induced oscillations of continuous systems with circular cross section", *J. Wind Eng. Ind. Aerod*., **14**, 431-442.
Tamura, Y. and Shimada, K. (1987), "A mathematical model for the transverse oscillations of square cylinders", *Proceedings of the 1st International Conference on Flow Induced Vibrations*, Bowness on Windermere, UK, May.
Vio, G.A., Dimitriadis, G. and Cooper, J.E. (2007), "Bifurcation analysis and limit cycle oscillation amplitude prediction methods applied to the aeroelastic galloping problem", *J. Fluids Struct*., 23(7), 983-1011.
Williamson, C. and Govardhan, R. (2008), "A brief review of recent results in vortex-induced vibrations", *J. Wind Eng. Ind. Aerod*., **96**(6-7), 713-735.

CC